

Article

## New Guanidine-Pyridine Copper Complexes and Their Application in ATRP

Alexander Hoffmann <sup>1</sup>, Olga Bienemann <sup>2</sup>, Ines dos Santos Vieira <sup>2</sup> and Sonja Herres-Pawlis <sup>1,\*</sup>

<sup>1</sup> Department Chemie, Ludwig-Maximilians-Universität München, Butenandtstr. 5-13, 81377 München, Germany; E-Mail: alexander.hoffmann@cup.uni-muenchen.de

<sup>2</sup> Anorganische Chemie II, Technische Universität Dortmund, Otto-Hahn-Str. 6, 44227 Dortmund, Germany; E-Mails: olga.bienemann@tu-dortmund.de (O.B.); ines.vieira@tu-dortmund.de (I.S.V.)

\* Author to whom correspondence should be addressed;

E-Mail: Sonja.Herres-Pawlis@cup.uni-muenchen.de; Tel.: +49 (0)89-2180-77486;

Fax: +49 (0)89-2180-77904.

Received: 27 February 2014; in revised form: 14 March 2014 / Accepted: 24 March 2014 /

Published: 1 April 2014

---

**Abstract:** The guanidine hybrid ligands, (tetramethylguanidine)methylenepyridine (TMGpy) and (dimethylethyleneguanidine)methylenepyridine (DMEGpy), were proven to be able to stabilize copper complexes active in the solvent-free polymerization of styrene at 110 °C using 1-phenylethylbromide as the initiator. The polymerization proceeded after first-order kinetics, and polystyrenes with polydispersities around 1.2 could be obtained. Using the ligand, DMEGpy, three new copper guanidine-pyridine complexes could be synthesized and structurally characterized. Their structural characteristics are discussed.

**Keywords:** copper complexes; hybrid guanidine ligands; X-ray; polymerization; ATRP

---

### 1. Introduction

Atom transfer radical polymerization (ATRP) is one of the most important and most efficient controlled radical polymerization methods, which combines the advantages of radical polymerization (high tolerance towards functional groups and impurities, many possible monomers and mild conditions) with the controlled character of a living polymerization. The living character of the controlled-radical polymerization methods can be obtained through suppression of termination and side reactions. This is achieved by a fast dynamic equilibrium between a very small number of

growing free radicals (active species) and a large number of non-reactive so-called dormant species [1]. Since the development of ATRP by K. Matyjaszewski in 1995, this field has run through a rapid progress in catalyst development, but also in the application to modern polymer technology [2,3]. In ATRP, the dormant species is an alkyl halide, which gives the active species after activation by atom transfer to a transition metal complex. Numerous transition metal systems on the basis of Cu, Fe, Ru and other transition metals of Groups 6 to 11 can be used, but Cu complexes dominate the field, due to the fast and clean polymerization. Mostly, polyfunctionalized N donor ligands are used for the stabilization of suited activator complexes [4]. Besides the classical ATRP, which starts with Cu(I), new ATRP methods have evolved that start with Cu(II) (e.g., Activators ReGenerated by Electron Transfer (ARGET) ATRP, Initiators for Continuous Activator Regeneration (ICAR)-ATRP [5,6] electrochemically mediated (e)ATRP [7,8]). Taking into account the idea of sustainability, intensive efforts have been undertaken to minimize the copper catalyst content. Here, there are still fundamental principles of the polymerization mechanism under discussion [9]. New ligands can significantly contribute to fundamental mechanistical understanding. Tailored ligand design enables the ideal adjustment of ligand properties to requests. By the choice of donor function and bridging units, the denticity and ligand geometry can be adapted, which steers the metal coordination and the redox potential. As donor functions, mainly amines, imines and pyridines have been tested [10].

Guanidines represent a further class of N donor ligands with a highly basic and nucleophilic imine function. The modular synthetic protocol allows for the combination of different spacers, amine groups and guanidine groups for building up a ligand library [11]. The donor properties can be tuned through the choice of guanidine substituents, amine and spacers. These ligands have already been intensely investigated in bioinorganic coordination chemistry [12–18], but also in the ATRP of styrene [19–24]. In all of these studies, it appeared that the polyfunctional guanidines support the oxidation state change from Cu(I) over Cu(II) to Cu(III) and stabilize the corresponding complexes excellently. These properties make guanidines ideal ligands for catalysis. Hybrid guanidines combine one guanidine function with one different donor function, e.g., pyridine or quinoline [13,17,18]. Here, we present three new copper guanidine-pyridine complexes and the first styrene ATRP studies with the hybrid guanidine ligands, (tetramethylguanidine)methylenepyridine (TMGpy) and (dimethylethyleneguanidine)methylenepyridine (DMEGpy).

## 2. Experimental Section

*General:* Ligand syntheses were performed under argon by using standard Schlenk techniques; complexes were prepared in a glove box under nitrogen atmosphere. Solvents were purified according to literature procedures and kept under nitrogen [25]. All chemicals were used as purchased, besides styrene, which was destabilized by eluting through a column of neutral Al<sub>2</sub>O<sub>3</sub>. The Vilsmeier salts, *N,N'*-dimethylethylenechloroformamidinium chloride (DMEG) and *N,N,N',N'*-tetramethylchloroformamidinium chloride (TMG), were synthesized as described in the literature [11,26]. The ligands DMEGpy and TMGpy were synthesized according to the protocol in the literature [27].

*Physical Methods:* The following spectrometers were used to record spectra. IR: FT-IR spectrometer IFS 28 from Bruker (Ettlingen, Germany). Mass spectra in the ESI-MS (Thermoquest

Finnigan, München, Germany) (4.5 kV, 350 °C) were recorded with a Thermoquest Finnigan. Elemental analysis: LECO-CHNS-932 (Leco, Mönchengladbach, Germany). NMR: Bruker DRX 400. The signals were calibrated to the residual signals of the deuterated solvent ( $\delta_{\text{H}}(\text{CDCl}_3) = 7.26$  ppm).

*Crystal Structure Analyses:* The crystal data for Compounds **1–3** are presented in Table 1. Data for these complexes were collected with an Xcalibur S diffractometer from Oxford Diffraction using Mo- $K_{\alpha}$  radiation ( $\lambda = 0.71073$  Å) and a graphite monochromator with the programs, CRYVALIS (Oxford Diffraction Ltd., Oxford, UK, 2008) and CRYVALIS RED (Oxford Diffraction Ltd., Oxford, UK, 2008). The structures were solved by direct methods (SHELXS90) [28] and conventional Fourier methods, and all non-hydrogen atoms refined anisotropically with full-matrix least-squares procedures based on  $F^2$  (SHELXL97) [29]. Hydrogen atoms were derived from difference Fourier maps and placed at idealized positions, riding on their parent carbon atoms, with isotropic displacement parameters  $U_{\text{iso}}(\text{H}) = 1.2U_{\text{eq}}(\text{C})$  and  $U_{\text{iso}}(\text{H}) = 1.5U_{\text{eq}}(\text{C methyl})$ . All methyl groups were allowed to rotate, but not to tip. CCDC-987045 (for **1**), CCDC-987046 (for **2**) and CCDC-987047 (for **3**) contain the supplementary crystallographic data for this paper. These data can be obtained free of charge from The Cambridge Crystallographic Data Centre (CCDC) [30].

*Gel Permeation Chromatography:* The average molecular weights and the weight distributions of the obtained polystyrene samples were determined by gel permeation chromatography (GPC) in THF as the mobile phase at a flow rate of 1 mL/min. The utilized GPCmax VE-2001 from Viscotek (Herrenberg, Germany) is a combination of an HPLC pump, an SDV column (PSS) with a porosity of 500 Å and a refractive index detector (VE-3580, Malvern, Herrenberg, Germany). The instrument was calibrated with standard polystyrene samples. Sample concentrations were 3 mg·mL<sup>-1</sup>.

*Synthesis of Copper Complexes:* To a solution of the copper starting compound (**1**: 0.5 mmol CuCl<sub>2</sub>, 67 mg; **2**: 0.5 mmol CuBr<sub>2</sub>, 112 mg; and **3**: 1 mmol CuCl<sub>2</sub>, 134 mg) and acetonitrile (1 mL) was added a solution of DMEGpy (1 mmol, 204 mg) in dry THF (1–2 mL), and the solution was stirred for 30 min. From the clear solution, crystals suitable for X-ray diffraction were obtained by slow diffusion of diethyl ether.

*[Cu(DMEGpy)<sub>2</sub>Cl][CuCl<sub>2</sub>] (1):* green crystals, yield: 0.353 mg (55%).

*IR* (KBr,  $\tilde{\nu}[\text{cm}^{-1}]$ ): 2924 w (v (CH<sub>arom</sub>)), 2877 w (v (CH<sub>aliph</sub>)), 1589 vs (v (C=N)), 1570 s (v (C=N)), 1508 w, 1479 m, 1435 m, 1400 m, 1358 w, 1294 m, 1281 m, 1230 w, 1107 vw, 1072 w, 1032 w, 964 w, 866 vw, 791 w, 771 w, 752 w, 656 vw, 627 vw, 577 vw, 550 vw, 482 vw. C<sub>22</sub>H<sub>32</sub>N<sub>8</sub>Cl<sub>3</sub>Cu<sub>2</sub> (641.99 g/mol), calcd. C 41.2; H 5.0; N 17.5; found C 40.8; H 5.1; N 17.2%. *ESI-MS* (DCM, m/z, (%)): 544.1 (10) [C<sub>22</sub>H<sub>32</sub>N<sub>8</sub>Cl<sub>2</sub>Cu + H<sup>+</sup>], 508.1 (<5) [C<sub>22</sub>H<sub>32</sub>N<sub>8</sub><sup>37</sup>Cl<sup>63</sup>Cu]<sup>+</sup> and [C<sub>22</sub>H<sub>32</sub>N<sub>8</sub><sup>35</sup>Cl<sup>65</sup>Cu]<sup>+</sup>, 506.1 (5) [C<sub>22</sub>H<sub>32</sub>N<sub>8</sub><sup>35</sup>Cl<sup>63</sup>Cu]<sup>+</sup>, 445.2 (16) [C<sub>22</sub>H<sub>32</sub>N<sub>8</sub> + 2H<sup>+</sup> + Cl<sup>-</sup>], 205.1 (100) [C<sub>11</sub>H<sub>16</sub>N<sub>4</sub> + H<sup>+</sup> = DMEGpy + H<sup>+</sup>].

*[Cu(DMEGpy)<sub>2</sub>Br][CuBr<sub>2</sub>] (2):* green crystals, yield: 0.504 mg (65%).

*IR* (KBr,  $\tilde{\nu}[\text{cm}^{-1}]$ ): 3041 vw (v (CH<sub>arom</sub>)), 2937 w (v (CH<sub>aliph</sub>)), 2875 w (v (CH<sub>aliph</sub>)), 593 vs (v (C=N)), 1567 s (v (C=N)), 1508 w, 1477 m, 1433 m, 1400 m, 1388 w, 1363 m, 1290 m, 1281 vw, 1232 m, 1151 w, 1108 w, 1076 w, 1056 w, 1036 m, 964 m, 895 vw, 864 w, 789 m, 777 m, 723 m, 650 w, 627 w, 581 w, 555 w, 478 w, 434 w. C<sub>22</sub>H<sub>32</sub>N<sub>8</sub>Br<sub>3</sub>Cu<sub>2</sub> (775.37 g/mol), calcd. C 34.1, H 4.2, N 14.5; found C 34.4, H 4.2, N 14.9%. *ESI(+)-MS* (MeOH, m/z, (%)): 552.1 (<5) [C<sub>22</sub>H<sub>32</sub>N<sub>8</sub>BrCu]<sup>+</sup>, 205.1 (100) [C<sub>11</sub>H<sub>16</sub>N<sub>4</sub> + H<sup>+</sup> = DMEGpy + H<sup>+</sup>].

*[Cu(DMEGpy)Cl<sub>2</sub>] (3):* green crystals, yield: 0.315 g (93%).

*IR* (KBr,  $\tilde{\nu}[\text{cm}^{-1}]$ ): 2948 vw (v (CH<sub>arom</sub>)), 2877 w (v (CH<sub>aliph</sub>)), 1589 vs (v (C=N)), 1570 s (v (C=N)),

1508 w, 1479 m, 1435 m, 1400 m, 1358 w, 1294 m, 1281 m, 1230 w, 1107 vw, 1072 w, 1032 w, 964 w, 866 vw, 791 w, 771 w, 752 w, 656 vw, 627 vw, 577 vw, 550 vw, 482 vw.  $C_{11}H_{16}N_4Cl_2Cu$  (338.72 g/mol), calcd. C 39.0, H 4.8, N 16.5; found C 39.2, H 4.7, N 16.7%. *ESI(+)-MS*: not soluble in a suitable solvent.

*Polymerization*: The components of catalysts for polymerization reactions containing the ligand (0.38 mmol, TMGpy: 78.4 mg or DMEGpy: 77.6 mg) and CuBr (0.19 mmol, 27.3 mg) were weighed in a Schlenk flask in a glove box. Outside the glove box, styrene (19 mmol, 2.2 mL) was added, and the mixture was degassed by three freeze-thaw cycles. Finally, the initiator, 1-PEBr (0.19 mmol, 35.2 mg, 26  $\mu$ L), was added through a syringe. The reaction mixture was heated in an oil bath at 110 °C, and samples (0.1 mL) were taken at different time intervals and quenched by cooling with liquid nitrogen. Monomer conversions were determined by  $^1H$  NMR spectroscopy (one drop in  $CDCl_3$ ), and molecular weight distributions were determined by GPC with the residual sample volume. For GPC analysis, this residual sample volume was eluted with THF (1.5 mL) through a column of neutral  $Al_2O_3$ .

**Table 1.** Crystallographic data and parameters.

	1	2	3
	[Cu(DMEGpy) <sub>2</sub> Cl][CuCl <sub>2</sub> ]	[Cu(DMEGpy) <sub>2</sub> Br][CuBr <sub>2</sub> ]	[Cu(DMEGpy)Cl <sub>2</sub> ]
Empirical formula	C <sub>22</sub> H <sub>32</sub> Cl <sub>3</sub> Cu <sub>2</sub> N <sub>8</sub>	C <sub>22</sub> H <sub>32</sub> Br <sub>3</sub> Cu <sub>2</sub> N <sub>8</sub>	C <sub>11</sub> H <sub>16</sub> Cl <sub>2</sub> CuN <sub>4</sub>
Form. mass/g·mol <sup>-1</sup>	641.99	775.37	338.72
Crystal Size/mm	0.25 × 0.13 × 0.12	0.22 × 0.11 × 0.07	0.13 × 0.09 × 0.04
T/K	173(2)	173(2)	173(2)
Crystal system	Triclinic	Monoclinic	Orthorhombic
Space group	$P\bar{1}$	C2/c	Pna2 <sub>1</sub>
a/Å	a = 11.265(1)	a = 22.783(2)	a = 8.783(1)
b/Å	b = 11.777(1)	b = 11.613(1)	b = 10.793(1)
c/Å	c = 12.135(1)	c = 22.834(3)	c = 14.605(1)
$\alpha$ /°	$\alpha$ = 114.5(1)	$\alpha$ = 90	$\alpha$ = 90
$\beta$ /°	$\beta$ = 104.1(1)	$\beta$ = 113.6(2)	$\beta$ = 90
$\gamma$ /°	$\gamma$ = 99.6(1)	$\gamma$ = 90	$\gamma$ = 90
V/Å <sup>3</sup>	1,354.0(2)	5,536.4(10)	1,384.5(2)
Z	2	8	4
$\rho_{calc.}/g/cm^3$	1.575	1.860	1.625
$\mu/mm^{-1}$	1.894	5.894	1.950
$\lambda/\text{Å}$	0.71073	0.71073	0.71073
F(000)	658	3,064	692
Range in hkl	±13, ±14, ±14	±27, -14 ≤ k ≤ 12, -26 ≤ l ≤ 27	±10, ±13, ±17
Reflections collected	13,335	15,612	12,453
Independent reflections	5,037	5,159	2,562
R <sub>int.</sub>	0.0344	0.0532	0.0494
Reflections observed	5,037	5,159	2,562
No. parameters	323	320	165
R <sub>1</sub> [I ≥ 2σ(I)]	0.0301	0.0338	0.0251
wR <sub>2</sub> (all data)	0.0631	0.0513	0.0415
Goodness-of-fit	0.893	0.854	0.893
Largest difference peak, hole/e·Å <sup>-3</sup>	0.332 and -0.535	0.957 and -0.803	0.502 and -0.277

### 3. Results and Discussion

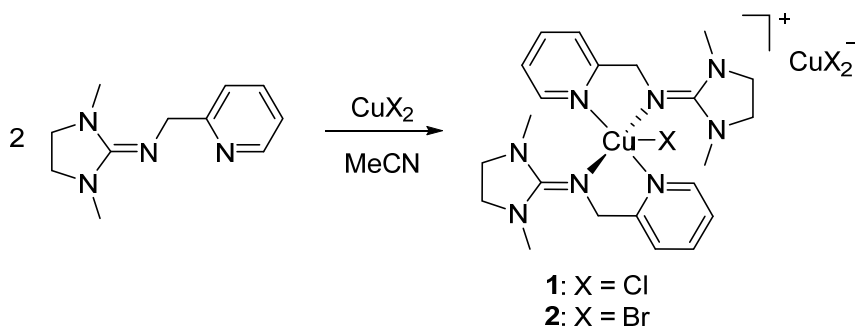
Ahead of polymerization experiments, we conducted complex synthesis and characterization experiments in order to structurally characterize our potential ATRP catalysts with the guanidine-pyridine ligands, TMGpy and DMEGpy, thoroughly. Hence, in Section 3.1, we firstly describe the complex syntheses of bis(chelate) and mono(chelate) copper guanidine-pyridine complexes together with their single crystal structure analyses and structural comparison to related copper complexes from the literature. With the ligand, TMGpy, we were not successful in preparation of single crystals. In Section 3.2, we describe then the ATRP experiments performed with the copper bromide catalyst species.

#### 3.1. Complex Synthesis

##### 3.1.1. Bis(chelate) Complexes **1** and **2**

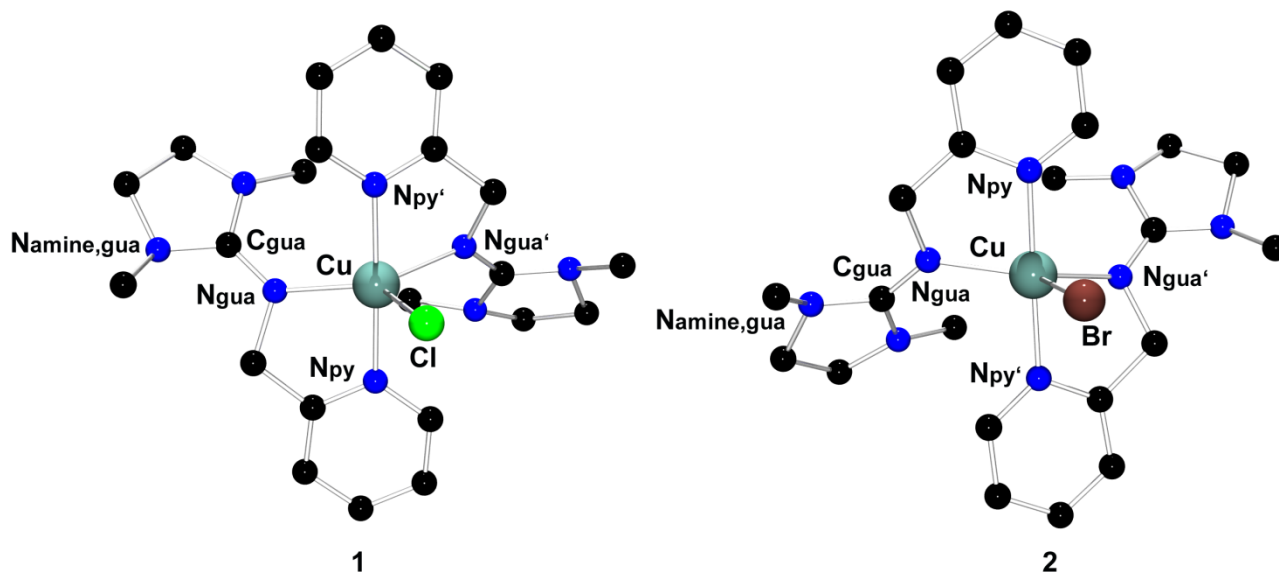
The reaction of two equivalents of DMEGpy with  $\text{CuCl}_2$  or  $\text{CuBr}_2$  yields the complexes,  $[\text{Cu}(\text{DMEGpy})_2\text{Cl}][\text{CuCl}_2]$  (**1**) and  $[\text{Cu}(\text{DMEGpy})_2\text{Br}][\text{CuBr}_2]$  (**2**) (Figure 1). **1** crystallizes in the triclinic space group  $P\bar{1}$ , and **2** in the monoclinic space group  $C2/c$ . In both complexes, the unit cell contains both isomers of the chiral cations. Selected geometrical data of these complexes are listed in Table 2.

**Figure 1.** Complex syntheses of  $[\text{Cu}(\text{DMEGpy})_2\text{Cl}][\text{CuCl}_2]$  (**1**) and  $[\text{Cu}(\text{DMEGpy})_2\text{Br}][\text{CuBr}_2]$  (**2**).



The complex cations in **1** and **2** are trigonal-bipyramidal polyhedra with the coordination of two DMEGpy ligands and one halide anion (Figure 2). As counterions, both complexes possess complex anions, namely  $\text{CuCl}_2^-$  (**1**) and  $\text{CuBr}_2^-$  (**2**), which are formed after the reduction of the copper(II) starting compound used. Presumably, the ligands serve as reductants. The observation of bromide anions in the ESI-MS spectra gives the hint that in solution, complexes with halide anions are present, as well.

**Figure 2.** Molecular structures of the complex cations,  $[\text{Cu}(\text{DMEGpy})_2\text{Cl}]^+$  and  $[\text{Cu}(\text{DMEGpy})_2\text{Br}]^+$ , in crystals of **1** and **2**.



The pyridine donors reside in the axial positions of the trigonal-bipyramidal coordination polyhedra, whereas the guanidine donors and the halide form the equatorial plane. The structural parameter,  $\tau_5$ , indicates the characteristic of such a polyhedron in distortion toward the square-pyramid (one being indicative of the trigonal-bipyramidal and zero for square-pyramid) [31]. The  $\tau_5$  values of 0.77 for **1** and 0.68 for **2** show that a distortion of the ideal trigonal-bipyramidal coordination occurs, which becomes clear in the increase in the equatorial angle,  $\text{N}_{\text{gua}}\text{-Cu-N}_{\text{gua}'}$ , with  $132.5(1)$  for **1** and  $136.9(2)$  for **2**. The  $\text{N}_{\text{py}}\text{-Cu-N}_{\text{py}'}$  angles do not deviate considerably from the ideal angle of  $180^\circ$  ( $178.6(1)$  for **1** and  $177.6(2)$  for **2**). The  $\text{Cu-N}_{\text{gua}}$  bond lengths in **1** and **2** ( $2.041(2)$ ,  $2.133(2)$  Å in **1**;  $2.029(4)$ ,  $2.065(3)$  Å in **2**) are longer than the  $\text{Cu-N}_{\text{py}}$  bond lengths ( $1.988(2)$ ,  $1.994(2)$  Å in **1**;  $1.991(4)$ ,  $1.993(1)$  Å in **2**). It is remarkable that the bonds to the axial ligands are shorter than those to the equatorial ligands [32,33]. The  $\text{Cu-N}_{\text{py}}$  bond lengths of both complexes are equal, whereas the  $\text{Cu-N}_{\text{gua}}$  bond lengths deviate significantly between **1** and **2**.

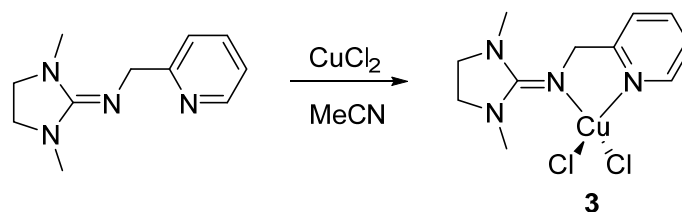
The structural parameter  $\rho$  can be used to evaluate in guanidines and their complexes the degree of delocalization of the guanidine moiety. The delocalization is important for effective coordination behavior towards metals in different oxidation states [18]. This parameter amounts in both complexes to 0.95, indicating a low charge delocalization within the  $\text{CN}_3$  guanidine framework. The intra-guanidine torsion is rather small, as expected for DMEG units, with  $\text{N}_{\text{amin, gua}}\text{C}_3\text{C}_{\text{gua}}\text{N}_3$  plane angles of  $14.7(\text{av})$  (**1**) and  $14.6(\text{av})$  (**2**) [12].

**Table 2.** Key geometric parameters of Complexes 1–3.

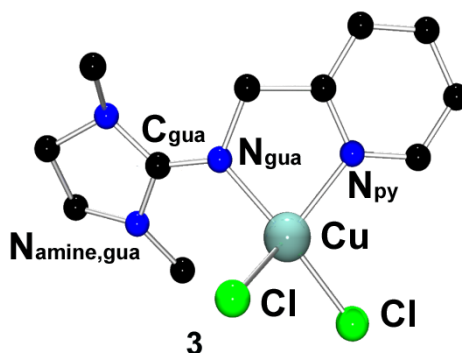
	1 [Cu(DMEGpy) <sub>2</sub> Cl][CuCl <sub>2</sub> ]	2 [Cu(DMEGpy) <sub>2</sub> Br][CuBr <sub>2</sub> ]	3 [Cu(DMEGpy)Cl <sub>2</sub> ]
<i>Bond lengths (Å)</i>			
Cu-N <sub>gua</sub>	2.041(2), 2.133(2)	2.029(4), 2.065(3)	1.956(3)
Cu-N <sub>py</sub>	1.988(2), 1.994(2)	1.991(4), 1.993(1)	2.016(3)
Cu-X	2.398(2)	2.589(1)	2.210(1), 2.243(1)
<i>Bond angles (°)</i>			
N <sub>gua</sub> -Cu-N <sub>py</sub>	81.3(1), 80.7(1)	81.7(2), 81.1(2)	81.7(1)
N <sub>gua</sub> -Cu-N <sub>gua'</sub>	132.5(1)	136.9(2)	
N <sub>py</sub> -Cu-N <sub>py'</sub>	178.6(1)	177.6(2)	
N <sub>gua</sub> -Cu-X	125.5(1), 102.1(1)	104.3(1), 118.8(1)	97.1(1), 152.6(1)
N <sub>py</sub> -Cu-X	89.8(1), 90.8(1)	87.5(1), 90.1(1)	98.0(1), 138.5(1)
X-Cu-X			100.8(1)
<i>Angles between planes (°)</i>			
∠(CuN <sub>ax</sub> , CuN <sub>eq</sub> )	85.2(1)	80.3(1)	
∠(CuN <sub>2</sub> , CuCl <sub>2</sub> )			48.3(1)
∠(N <sub>amine, gua</sub> C <sub>3</sub> , C <sub>gua</sub> N <sub>3</sub> )	14.7(av)	14.6(av)	14.8(av)
<i>Structural parameter ρ and τ<sub>5</sub></i>			
ρ	0.95	0.95	0.95
τ <sub>5</sub>	0.77	0.68	0.49

### 3.1.2. Mono(chelate) Complex 3

The reaction of one equivalent of DMEGpy with one equivalent of CuCl<sub>2</sub> gives the mono(chelate) complex, [Cu(DMEGpy)Cl<sub>2</sub>] (**3**) (Figure 3). This complex crystallizes in the orthorhombic space group *Pna*2<sub>1</sub>. Selected geometrical data of this complex are listed in Table 2.

**Figure 3.** Synthesis of the complex, [Cu(DMEGpy)Cl<sub>2</sub>] (**3**).

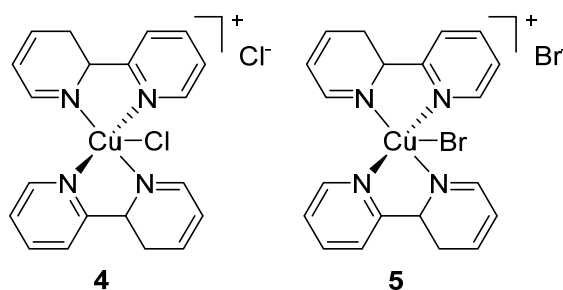
The molecular structure of **3** is depicted in Figure 4. **3** is a four-coordinate complex with the coordination by one bidentate ligand and two chloride anions. Here, the τ<sub>4</sub>-value can give a measurement of the degree of distortion between tetrahedral and square-planar coordination (square-planar: zero; tetrahedral: one) [34]. With a τ<sub>4</sub>-value of 0.49, the observed coordination geometry of **3** lies in the middle between both polyhedra. This is in accordance with the angle between the CuN<sub>2</sub>- and the CuCl<sub>2</sub>-planes of 48.3(1).

**Figure 4.** Molecular structure of  $[\text{Cu}(\text{DMEGpy})\text{Cl}_2]$  (**3**) in the solid state.

The Cu-N<sub>gua</sub> bond is with 1.956(3) Å considerably shorter than the Cu-N<sub>py</sub> bond (2.016(3) Å). The  $\rho$ -value of 0.95 shows a small degree of charge delocalization within the guanidine unit. The intra-guanidine torsion is small (14.8°(av)), as expected for a DMEG unit [12].

### 3.1.3. Comparative Structural Discussion

In this section, we compare the presented complexes, **1** and **2**, with five-coordinate copper(II) complexes with the symmetric ligand, 2,2'-bipyridine (bpy):  $[\text{Cu}(\text{bpy})_2\text{Cl}]\text{Cl}\cdot 6\text{H}_2\text{O}$  (**4**) [35] and  $[\text{Cu}(\text{bpy})_2\text{Br}]\text{Br}$  (**5**) [36] (Figure 5 and Table 3).

**Figure 5.** Comparative complexes  $[\text{Cu}(\text{bpy})_2\text{Cl}]\text{Cl}\cdot 6\text{H}_2\text{O}$  (**4**) [35] and  $[\text{Cu}(\text{bpy})_2\text{Br}]\text{Br}$  (**5**) [36].**Table 3.** Key geometric parameters of **4** [35] and **5** [36].

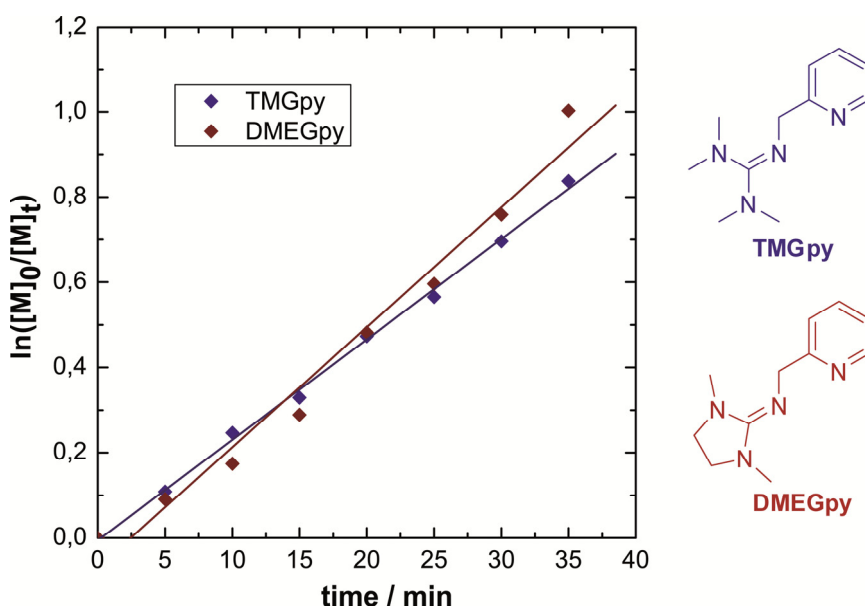
	<b>4</b> $[\text{Cu}(\text{bpy})_2\text{Cl}]\text{Cl}\cdot 6\text{H}_2\text{O}$	<b>5</b> $[\text{Cu}(\text{bpy})_2\text{Br}]\text{Br}$
<i>Bond lengths (Å)</i>		
Cu-N <sub>ax</sub>	1.989(10), 1.970(10)	1.977(6), 1.978(6)
Cu-N <sub>eq</sub>	2.077(10), 2.087(10)	2.075(8), 2.085(7)
Cu-X	2.361(4)	2.429(2)
<i>Bond angles (°)</i>		
N-Cu-N	79.3(4), 79.8(4)	80.4(3), 80.3(3)
N <sub>ax</sub> -Cu-N <sub>ax</sub>	178.3(4)	177.3(3)
N <sub>eq</sub> -Cu-Cl	118.7(3), 118.6(3)	128.6(2), 124.7(2)
N <sub>eq</sub> -Cu-N <sub>eq</sub>	122.8(4)	106.7(3)
<i>Structural parameter <math>\tau_5</math></i>		
$\tau_5$	0.93	0.81

The bonds to the axial ligands are shorter than the bonds to the equatorial ligands in the guanidine-pyridine complexes, **1** and **2**, as well as in the comparative bipyridine complexes, **4** and **5**. Hence, the metal bonding influence is as strong as the donor difference. The angles of the coordination polyhedra of **4** and **5** are very similar to those of **1** and **2**. Interestingly, the Cu-halide distances in **1** and **2** are longer than those in **4** and **5**, which might be indicative of the larger donor strength of the guanidine functions.

### 3.2. Atom Transfer Radical Polymerization of Styrene

The ligands, TMGpy and DMEGpy, together with CuBr as the copper source, have been investigated towards their activity in styrene ATRP with the initiator 1-phenylethylbromide (PEBr). The ratio of styrene/ligand/CuBr/PEBr was 100/2/1/1. The reaction temperature was 110 °C, and samples were drawn in equidistant time intervals and plotted semilogarithmically (Figure 6). It has to be noted that the polymerization occurs in a homogeneous solution of the *in situ* formed complexes in the styrene bulk. The styrene-ATRP with the catalysts **2**, TMGpy/CuBr and 2 DMEGpy/CuBr, follows a first-order kinetics, which indicates a constant radical concentration and, thus, the living character of the polymerization. After a polymerization time of 35 min, the conversion reaches a value of 57% with 2 TMGpy/CuBr and of 63% with 2 DMEGpy/CuBr. The apparent rate constant ( $k_{app}$ ) amounts to  $4.20 \times 10^{-4} \text{ s}^{-1}$  (2 TMGpy/CuBr) and  $4.69 \times 10^{-4} \text{ s}^{-1}$  (2 DMEGpy/CuBr). Hence, we can detect only a small amount of activity difference between the two guanidine complexes. The polymerization speed is high compared to related systems with pyridine-based copper catalysts, such as CuBr/2bipy or CuBr/2dNBipy, which mediate a significantly slower polymerization [37]. Moreover, the bipy system was reported to proceed under heterogeneous conditions [37].

**Figure 6.** The semilogarithmic plot of the conversion against time for the styrene atom transfer radical polymerization (ATRP) mediated by 2 (tetramethylguanidine)methylenepyridine (TMGpy) (blue)/2 DMEGpy (red) and CuBr and 1-phenylethylbromide (PEBr) as the initiator at 110 °C. The ratio of styrene:ligand:CuBr:PEBr = 100:2:1:1.

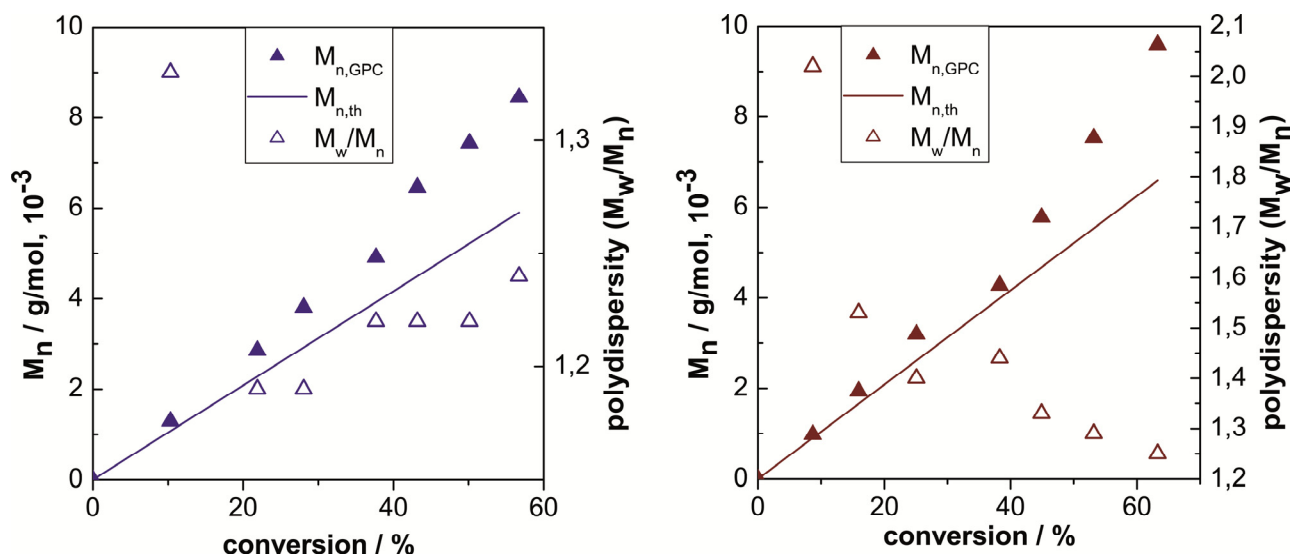


The progress of the polymerization as marked by the development of the molecular weight and the polydispersities is depicted in Figure 7. Selected polymerization data are given in Table 4.

**Table 4.** Conversion,  $M_{n,GPC}$ ,  $M_{n,th}$  and  $M_w/M_n$  for the kinetics of styrene ATRP with 2 TMGpy/CuBr and 2 DMEGpy/CuBr and PEBr at 110 °C after 10 and 35 min.

Catalyst	t (min)	Conversion (%)	$M_{n,GPC}$ (g/mol)	$M_{n,th}$ (g/mol)	$M_w/M_n$
2 TMGpy/CuBr	10	22	2900	2200	1.19
2 TMGpy/CuBr	35	57	8500	4900	1.24
2 DMEGpy/CuBr	10	16	1900	1700	1.53
2 DMEGpy/CuBr	35	63	9600	6600	1.25

**Figure 7.** Progress of the number-averaged molecular weights ( $M_{n,GPC}$ ), the theoretical molecular weight ( $M_{n,th}$ ) and the polydispersity with the conversion for styrene ATRP with: (left) 2 TMGpy and CuBr; (right) 2 DMEGpy and CuBr; and PEBr as the initiator at 110 °C. The ratio of styrene:ligand:CuBr:PEBr = 100:2:1:1.



For both polymerizations, the average molecular weights increase linearly, but deviate significantly from the theoretical molecular weights at conversion >40%. The initiator efficiency can be calculated as the slope of the linear function of  $M_{n,th}$  vs.  $M_{n,GPC}$  [38]. Here, it points towards a small deactivation rate ( $f_{TMGpy} = 0.72$ ;  $f_{DMEGpy} = 0.76$ ). The polydispersities decrease during polymerization with 2 TMGpy/CuBr to values under 1.2 and increase again to 1.24, indicating a loss of control by the small deactivation rate. Using 2 DMEGpy/CuBr, the polydispersity only decreases to a value of 1.24. In summary, the catalysts, 2 TMGpy/CuBr and 2 DMEGpy/CuBr, show a high activity. Due to small deviations of the averaged and theoretical molecular weights and the small polydispersities, the polymerization control can be rated as medium. We relate the increase in polymerization speed to the changed donor situation of the copper complexes with one guanidine and one pyridine donor combined within the ligands.

#### 4. Conclusions

Herein, we report three new guanidine-pyridine copper(II) complexes. The bis(chelate) complexes, **1** and **2**, exhibit trigonal-bipyramidal coordination geometries with axial pyridine donors and equatorial guanidine and halide ligands. The bonds to the pyridine donors are slightly shorter than to the guanidine donors. Overall, the guanidine donor seems to be the stronger donor, as was shown in the mono(chelate) complex, **3**, with considerably shorter Cu-N<sub>gua</sub> bonds. The corresponding guanidine-pyridine ligands were shown to mediate with their copper complexes controlled by styrene ATRP. Remarkably and in contrast to the bipy systems, the polymerization mixture stayed homogeneous. The polymerization proceeds considerably faster than with dNbipy/2CuBr, but with a smaller degree of control.

#### Acknowledgments

The authors thank the Deutsche Forschungsgemeinschaft (FOR1405) for financial support. Moreover, Sonja Herres-Pawlis and Olga Bienemann gratefully acknowledge the Fonds der Chemischen Industrie for fellowships.

#### Author Contributions

Olga Bienemann synthesized the ligands and complexes and performed the polymerization studies. Ines dos Santos Vieira collected and analyzed the X-ray data. Alexander Hoffmann and Sonja Herres-Pawlis wrote the manuscript.

#### Conflicts of Interest

The authors declare no conflict of interest.

#### References

1. Matyjaszewski, K.; Davis, T.P. *Handbook of Radical Polymerization*; Wiley Interscience: Hoboken, NJ, USA, 2002.
2. Wang, J.-S.; Matyjaszewski, K. Controlled/“living” radical polymerization. Atom transfer radical polymerization in the presence of transition-metal complexes. *J. Am. Chem. Soc.* **1995**, *117*, 5614–5615.
3. Patten, T.E.; Matyjaszewski, K. Atom Transfer Radical Polymerization and the Synthesis of Polymeric Materials. *Adv. Mater.* **1998**, *10*, 901–915.
4. Matyjaszewski, K.; Xia, J. Atom Transfer Radical Polymerization. *Chem. Rev.* **2001**, *101*, 2921–2990.
5. Jakubowski, W.; Matyjaszewski, K. Activators Regenerated by Electron Transfer for Atom-Transfer Radical Polymerization of (Meth)acrylates and Related Block Copolymers. *Angew. Chem. Int. Ed.* **2006**, *45*, 4482–4486.
6. Matyjaszewski, K.; Jakubowski, W.; Min, K.; Tang, W.; Huang, J.; Braunecker, W.A.; Tsarevsky, N.V. Diminishing catalyst concentration in atom transfer radical polymerization with reducing agents. *Proc. Natl. Acad. Sci. USA* **2006**, *103*, 15309–15314.

7. Magenau, A.J.D.; Strandwitz, N.C.; Gennaro, A.; Matyjaszewski, K. Electrochemically Mediated Atom Transfer Radical Polymerization. *Science* **2011**, *332*, 81–84.
8. Bortolamei, N.; Isse, A.A.; Magenau, A.J.D.; Gennaro, A.; Matyjaszewski, K. Controlled Aqueous Atom Transfer Radical Polymerization with Electrochemical Generation of the Active Catalyst. *Angew. Chem. Int. Ed.* **2011**, *50*, 11391–11394.
9. Konkolewicz, D.; Wang, Y.; Zhong, M.; Kryszewski, P.; Isse, A.A.; Gennaro, A.; Matyjaszewski, K. Reversible-Deactivation Radical Polymerization in the Presence of Metallic Copper. A Critical Assessment of the SARA ATRP and SET-LRP Mechanisms. *Macromolecules* **2013**, *46*, 8749–8772.
10. Tang, W.; Kwak, Y.; Braunecker, W.; Tsarevsky, N.V.; Coote, M.L.; Matyjaszewski, K. Understanding Atom Transfer Radical Polymerization: Effect of Ligand and Initiator Structures on the Equilibrium Constants. *J. Am. Chem. Soc.* **2008**, *130*, 10702–10713.
11. Herres-Pawlis, S.; Neuba, A.; Seewald, O.; Seshadri, T.; Egold, H.; Flörke, U.; Henkel, G. A library of peralkylated bisguanidine ligands for use in biomimetic coordination chemistry. *Eur. J. Org. Chem.* **2005**, *2005*, 4879–4890.
12. Herres-Pawlis, S.; Flörke, U.; Henkel, G. Tuning of Copper(I)-Dioxygen Reactivity by Bisguanidine Ligands. *Eur. J. Inorg. Chem.* **2005**, *2005*, 3815–3824.
13. Wortmann, R.; Hoffmann, A.; Haase, R.; Flörke, U.; Herres-Pawlis, S. Synthese und Charakterisierung von Cobalt(II)- und Kupfer(I)-Komplexen mit Guanidin-Pyridin-Hybridliganden. *Z. Anorg. Allg. Chem.* **2009**, *635*, 64–69.
14. Herres-Pawlis, S.; Haase, R.; Henkel, G.; Binder, S.; Eich, A.; Schulz, B.; Rübhausen, M.; Wellenreuther, G.; Meyer-Klaucke, W. Stabilisation of a Highly Reactive Bis-( $\mu$ -oxo)dicopper(III) Species at Room Temperature by Electronic and Steric Constraint of an Unconventional Nitrogen Donor Ligand. *Chem. Eur. J.* **2009**, *35*, 8678–8682.
15. Herres-Pawlis, S.; Seshadri, T.; Flörke, U.; Henkel, G. Reactivity of 2,2'-Bis(2N-(1,1',3,3'-tetramethyl-guanidino))diphenylene-amine with CuI and [Cu(MeCN)<sub>4</sub>][PF<sub>6</sub>]: benzimidazole formation vs. Cu oxidation. *Z. Anorg. Allg. Chem.* **2009**, *635*, 1209–1214.
16. Herres-Pawlis, S.; Berth, G.; Wiedemeier, V.; Schmidt, L.; Zrenner, A.; Warnecke, H.-J. Oxygen sensing by fluorescence quenching of [Cu(btmgp)I]. *J. Lumin.* **2010**, *130*, 1958–1962.
17. Haase, R.; Beschnitt, T.; Flörke, U.; Herres-Pawlis, S. Bidentate guanidine ligands with ethylene spacer in copper-dioxygen chemistry: Structural characterization of bis(l-hydroxo) dicopper complexes. *Inorg. Chim. Acta* **2011**, *374*, 546–557.
18. Bienemann, O.; Hoffmann, A.; Herres-Pawlis, S. (Guanidine)copper complexes: structural variety and application in bioinorganic chemistry and catalysis. *Rev. Inorg. Chem.* **2011**, *3*, 83–108.
19. Petrovic, D.; Hill, L.M.R.; Jones, P.G.; Tolman, W.B.; Tamm, M. Synthesis and reactivity of copper(I) complexes with an ethylene-bridged bis(imidazolin-2-imine) ligand. *Dalton Trans.* **2008**, *7*, 887–894.
20. Oakley, S.H.; Coles, M.P.; Hitchcock, P.B. Structural and catalytic properties of bis(guanidine)copper(I) halides. *Inorg. Chem.* **2003**, *42*, 3154–3156.
21. Brar, A.S.; Kaur, S. Tetramethylguanidino-tris(2-aminoethyl)amine: A novel ligand for copper-based atom transfer radical polymerization. *J. Polym. Sci. A Polym. Chem.* **2005**, *43*, 5906–5922.
22. Bienemann, O.; Haase, R.; Flörke, U.; Döring, A.; Kuckling, D.; Herres-Pawlis, S. Neue Bisguanidin-Kupfer-Komplexe und ihre Anwendung in der ATRP. *Z. Naturforsch.* **2010**, *65b*, 798–806.

23. Bienemann, O.; Haase, R.; Jesser, A.; Beschnitt, T.; Döring, A.; Kuckling, D.; dos Santos Vieira, I.; Flörke, U.; Herres-Pawlis, S. Synthesis and Application of new Guanidine Copper Complexes in Atom Transfer Radical Polymerisation. *Eur. J. Inorg. Chem.* **2011**, *2011*, 2367–2379.
24. Bienemann, O.; Froin, A.-K.; dos Santos Vieira, I.; Wortmann, R.; Hoffmann, A.; Herres-Pawlis, S. Structural Aspects of Copper-Mediated Atom Transfer Radical Polymerisation with a Novel Tetradentate Bisguanidine Ligand. *Z. Anorg. Allg. Chem.* **2012**, *638*, 1683–1690.
25. Leonard, J.; Lygo, B.; Procter, G. *Praxis der Organischen Chemie*; Wiley-VCH: Weinheim, Germany, 1996.
26. Kantlehner, W.; Haug, E.; Mergen, W.W.; Speh, P.; Maier, T.; Kapassakalidis, J.J.; Bräuner, H.-J.; Hagen, H.; Orthoamide, X.L. Herstellung von 1,1,2,3,3-pentasubstituierten und 1,1,2,2,3,3-hexasubstituierten Guanidiniumsalzen sowie von 1,1,2,3,3-Pentaalkylguanidinen. *Liebigs Ann. Chem.* **1984**, *1*, 108–125.
27. Hoffmann, A.; Börner, J.; Flörke, U.; Herres-Pawlis, S. Synthesis and fluorescence properties of guanidine-pyridine hybridligands and structural characterisation of their mono- and bis(chelated) cobalt complexes. *Inorg. Chim. Acta* **2009**, *362*, 1185–1193.
28. Sheldrick, G.M. Phase annealing in SHELX-90: Direct methods for larger structures. *Acta Crystallogr.* **1990**, *A46*, 467–473.
29. Sheldrick, G.M. *SHELXL*; University of Göttingen: Göttingen, Germany, 1997.
30. CCDC CIF Depository Request Form. Available online: [http://www.ccdc.cam.ac.uk/data\\_request/cif](http://www.ccdc.cam.ac.uk/data_request/cif) (accessed on 27 March 2014).
31. Addison, A.W.; Rao, T.N.; Reedik, J.; van Rijn, J.; Verschoor, G.C. Synthesis, Structure, and Spectroscopic Properties of Copper(II) Compounds containing Nitrogen-Sulphur Donor Ligands; the Crystal and Molecular Structure of Aqua[1,7-bis(N-methylbenzimidazol-2'-yl)-2,6-dithiaheptane]copper(II) Perchlorate. *J. Chem. Soc. Dalton Trans.* **1984**, *1984*, 1349–1356.
32. Gispert, J.R. *Coordination Chemistry*; Wiley-VCH: Weinheim, Germany, 2008.
33. Rossi, A.R.; Hoffmann, R. Transition metal pentacoordination. *Inorg. Chem.* **1975**, *14*, 365–374.
34. Yang, L.; Powell, D.R.; Houser, R.P. Structural variation in copper(I) complexes with pyridylmethylamide ligands: structural analysis with a new four-coordinate geometry index,  $\tau_4$ . *Dalton Trans.* **2007**, *2007*, 955–964.
35. Stephens, F.S.; Tucker, P.A. Crystal and molecular structure of chlorobis(2,2'-bipyridyl)copper(II) chloride hexahydrate. *J. Chem. Soc. Dalton Trans.* **1973**, *1973*, 2293–2297.
36. Khan, M.A.; Tucker, D.G. Structure of bis(2,2'-bipyridine)monobromocopper(II) bromide. *Acta Cryst.* **1981**, *B37*, 1409–1412.
37. Matyjaszewski, K.; Patten, T.E.; Xia, J. Controlled/"Living" Radical Polymerization. Kinetics of the Homogeneous Atom Transfer Radical Polymerization of Styrene. *J. Am. Chem. Soc.* **1997**, *119*, 674–680.
38. Poli, R. Relationship between One-Electron Transition-Metal Reactivity and Radical Polymerization Processes. *Angew. Chem. Int. Ed.* **2006**, *45*, 5058–5070.